Fermi National Accelerator Laboratory

FERMILAB-Pub-77/95-THY
October 1977

A Determination of the Sea Quark Distributions in the Proton by Single Particle Inclusive Reactions

DENNIS W. DUKE
Fermi National Accelerator Laboratory, Batavia, Illinois 60510*

and

FRANK E. TAYLOR
Northern Illinois University, DeKalb, Illinois 60174

ABSTRACT

We have determined the sea quark distributions of the proton by using recent data on meson production in the proton fragmentation region in high energy proton-proton collisions. We find that the magnitude of the sea distributions in hadron reactions is larger than the sea measured in lepton experiments. We interpret this enhancement as due to the additional contribution of quark-antiquark pairs created in the initial hadron collision. From our determination of the sea quark distributions we are able to predict a number of particle ratios in single particle inclusive production in p-p collisions. In addition, we have calculated the production cross section for low mass muon-pairs by the Drell-Yan mechanism and have obtained good agreement with experiment.

* Operated by Universities Research Association Inc. under contract with the Energy Research and Development Administration

I. INTRODUCTION

Deep inelastic lepton-nucleon scattering data allows one to determine the up (u(x)) and the down (d(x)) quark distributions within the proton. However these data do not permit an equally precise determination of the sea quark distributions.[1] Forthcoming data on the production of high mass muon pairs interpreted by the Drell-Yan model should provide a determination of the sea quark distributions averaged over quark flavors, but will not allow the sea quark distributions for individual flavors to be ascertained.

Recent phenomenological work applying the quark-parton model to single hadron inclusive production in high energy p-p collisions in the low p_T region has been done.[2,3] This empirically motivated work employs a quark recombination model which permits the effective sea quark distributions to be determined with a greater sensitivity than that of deep inelastic lepton scattering. We have used this model and recent data[4] on inclusive single meson production in p-p collisions in the proton fragmentation region to determine the sea quark distributions in the proton.

In Section II the quark recombination model is reviewed. Our determination of the sea quark distributions is presented in Section III. With these sea quark distributions, we give predictions for various additional particle ratios in Section IV. In Section V we discuss our results, and a summary is presented in Section VI.

II. QUARK RECOMBINATION IN THE FRAGMENTATION REGION

Ochs has demonstrated[2] a striking empirical similarity between the measured π^+/π^- ratio in the proton fragmentation region of p-p collisions and the u/d quark ratio measured by deep-inelastic lepton scattering. This observation implies that in π^+ production in p-p collisions, the u quark in a fast π^+ should be one of the original valence u quarks in the incident proton. Similar arguments hold for the d quark in π^- production. Hence low p_T single hadron production at high energies gives information on the constituent structure of the initial protons in p-p collisions.

It is widely believed that hadron production in e^+e^- colliding beam reactions and deep inelastic lepton reactions in the current fragmentation region proceeds via a quark fragmentation mechanism.[1] (See Fig. 1a). Das and Hwa[3] were able to calculate the absolute magnitude of this process and have shown that quark fragmentation cannot contribute more than about 1% of the single meson production cross section at low p_T and large x. This result led them to consider a quark recombination mechanism[5] for single meson production. In this quark recombination model, a pion produced at large x should be initiated by a quark whose momentum is also large. Since only valence quarks are believed to have a significant probability for being found at large x, the high momentum quark in pion production must be one of

the valence quarks of the initial hadron. This fast quark then picks up a slow antiquark from the sea by a quark-antiquark recombintation process to emerge as a meson (Fig. 1(b)). Hence single pion inclusive production at large x and small p_T is sensitive to the probability for finding a quark-antiquark pair with the right quantum numbers.

In the model of Das and Hwa[3] the x distribution of single meson production is given by

$$H_M(x) = \int \frac{dx_1}{x_1} \int \frac{dx_2}{x_2} \; F(x_1, x_2) \; R(x_1, x_2, x), \tag{1}$$

where x_1 and x_2 are the q and $\bar{q}$ x-values, $F(x_1, x_2)$ is the $q-\bar{q}$ joint momentum probability distribution function and $R(x_1, x_2, x)$ is the $q-\bar{q}$ recombination function. Das and Hwa assume

$$F(x_1, x_2) = F_q(x_1) \; F_{\bar{q}}(x_2) \; \beta_M(1 - x_1 - x_2), \tag{2}$$

where for example $F_u(x) = x\,u(x)$ is the u-quark momentum probability distribution, and $\beta_M(1 - x_1 - x_2)$ is a phase space factor. They also take

$$R(x_1, x_2, x) = \alpha_M \; \frac{x_1}{x} \; \frac{x_2}{x} \; \delta\left(1 - \frac{x_1}{x} - \frac{x_2}{x}\right) . \tag{3}$$

With these assumptions, one obtains

$$H_M(x) = \alpha_M \beta_M \frac{1-x}{x} \int_0^x dx_1 \, F_q(x_1) \, F_{\bar{q}}(x-x_1) \, . \qquad (4)$$

Clearly several approximations are involved in Eqs. (2) and (3). In particular the phase space factor $\beta_M(1-x_1-x_2)$ can only be approximately correct, since it does not allow the joint quark distribution to be integrated to regain the known single quark distributions.[6] We reduce our sensitivity to this approximation by focusing our analysis on particle production ratios where the phase space factors cancel.

The constraint $x=x_1+x_2$, expressed by the delta function in Eq. (3), implies that the recombination is exclusively a two-body process. As noted by Das and Hwa,[3] this assumption does not mean that the final observed pion does not contain sea partons. Presumably the pion sea is built in a relatively long time interval after the recombination. We expect the contribution of many-body recombination to be small, except for x very near 1, when it leads to the Regge behavior.[6] For reference we have listed in Table I formulas for tne explicit particle ratios that we use in our analysis. We note for example that the π^+/π^- ratio depends on the ratio of the integrals

$$\int_0^x F_u(x_1) \, F_{\bar{d}}(x-x_1) \, dx_1 \Big/ \int_0^x F_d(x) \, F_{\bar{u}}(x-x_1) \, dx_1 .$$

Hence for a steeply falling sea distribution, the ratio of these integrals became approximately $\sim F_u(x)F_{\bar{d}}(o)/F_d(x)F_{\bar{u}}(o) \sim u(x)/d(x)$. Hence, we regain the empirical observation of Ochs.[2]

III. DETERMINATION OF THE SEA-QUARK DISTRIBUTIONS

The procedure which we used for determining the sea quark distributions $F_{\bar{u}}(x)$, $F_{\bar{d}}(x)$, $F_s(x)$, and $F_{\bar{s}}(x)$ was to fit the data on four particle production ratios to the functions given in Table I. We begin by making several plausible assumptions in the model of Das and Hwa.

1. We take the phase space constants β_M to be equal and therefore independent of the particle species. (We also take the phase space dependence $(1 - x_1 - x_2)$ for each particle species).

2. We assume the constants α_M to be equal and hence take the quark-antiquark recombination process to be independent of particular flavor combinations.

3. For the functions $F_u(x) = x\,u(x)$ and $F_d(x) = xd(x)$ we use the Field and Feynman valence quark distributions[1] plus our own sea quark distributions. We have done this by subtracting the Field-Feynman sea distributions from their fits to xu(x) and xd(x) and adding our own sea distributions to this. We adopt a simple form for the sea distributions, namely $xu(x) - x\bar{u}(x) = u_o(1-x)^{n_u}$, $xd(x) = x\bar{d}(x) = d_o(1-x)^{n_d}$, and $xs(x) = x\bar{s}(x) = s_o(1-x)^{n_s}$. We therefore have the constants u_o, d_o, s_o and the exponents n_u, n_d, and n_s to determine using the particle ratio data.

Let us consider what magnitude to expect for the constants u_o, d_o and s_o. For the quiescent proton probed by the photon in deep-inelastic lepton scattering, these constants are known to lie in the approximate

range 0.1-0.3. However we also know from the momentum sum rules that approximately 50% of the momentum of the proton is carried by neutral partons, presumably (colored) vector gluons. These gluons must contribute in some major way to the meson production. There are essentially two possibilities:

1. The gluons fragment directly to mesons (Fig. 1c). This process must be similar in magnitude to quark fragmentation, and hence is ruled out be the data.

2. The gluons create $q\bar{q}$ pairs in the proton sea, and the recombination mechanism gradually depletes this enhanced sea population as illustrated in Fig. 1d. In this manner all the momentum in the neutral partons is eventually converted to sea $q\bar{q}$ pairs and hence to mesons. Clearly the time scale for this rearrangement must be fairly long. Thus we might expect to find the constants u_o, d_o, and s_o of sufficient magnitude to account for nearly all of the proton momentum. Indeed, we will show that the data actually forces us to this conclusion.

In Fig. 2 we have plotted the π^+/π^- ratios from FERMILAB[4] and ISR[7,8] as a function of the radial variable x_R defined as E^*/E^*_{max}, where E^* = energy of the detected particle in the c.m. frame and E^*_{max} = maximum energy available to that particle in the c.m. frame. The invariant cross sections for single particle inclusive reactions have been shown to scale over a wider range when this scaling variable is used then when the Feynman scaling variable $x_{||} = 2P^*_{||}/\sqrt{s}$ is used.[9]

However, since we are concerned with the low p_T-high energy region $x_R \approx |x_{||}|$, and our results are not sensitive to the distinction between $x_{||}$ and x_R in this kinematic range.

Referring to Table I, we see that for large x the magnitude of the π^+/π^- ratio is controlled by the d_o/u_o ratio, and the shape is controlled by n_d and n_u. The curves shown in Fig. 2 are obtained by taking $u_o=d_o$ (consistent with the isosinglet nature of the Pomeron) and various values of $n_u=n_d$. We see that $n_u=n_d=8\pm1$ gives an adequate fit.

Although the parameters n_u and n_d are determined quite precisely by the data under our simplifying assumptions, our results may systematically be changed by using other parametrizations of the valence quark distributions.[10] For example, a parameterization constraining $xd(x) \sim (1-x)^5$ for large x lowers the best fit value of $n_u=n_d$ by 1 unit.

Recent measurements[11] at the ISR of the π^+/π^- ratio have yielded results somewhat larger than the data of Johnson et al.[4] We find that the values $n_u=n_d=10$ will accommodate the ISR data. However, we stress that for a given set of data and valence quark distributions, our method allows a very precise determination of the sea quark distributions.

Now consider the K^+/K^- ratio shown in Fig. 3. Referring to Table I, we see that the magnitude of the ratio depends on u_o and the shape depends on n_s if we consider $n_u=n_d=8$ fixed by the π^+/π^- ratio.

A good fit is obtained by setting $u_o=d_o=1.2$ and $n_s=5.75$. We estimate the uncertainty in u_o to be no more than ± 10%. The data favor a value of n_s less than $n_u=n_d$, although the case $n_s=n_u=n_d$ cannot be definitely ruled out.

The π^-/K^- ratio is shown in Fig. 4. Referring to Table I, we see that the shape of this ratio is determined by the relative shapes of the d and s quark structure functions. Since the π^-/K^- ratio rises with increasing x, it follows that $n_s > 4$. The value $n_s=5.75$ determined above adequately describes the ratio if we take $s_o=0.135$ (±0.015).

We have plotted the data and theory for the π^+/K^+ ratio in Fig. 5, although both are entirely determined by the previous three ratios. Nevertheless it is interesting to observe the fall of the ratio with increasing x_R. This decrease of the calculated π^+/K^+ ratio is due to $n_s<n_u=n_d$.

A note of caution is necessary concerning the π/K ratios. Data at higher p_T [12] show smaller values of these ratios than data at low p_T, and therefore these ratios are not functions of x_R(or $x_{||}$) alone. We have therefore restricted ourselves to fitting data on the π/K ratios at only low p_T. Furthermore, it is clear that resonances may also affect the π/K ratios at small x_R. These effects are discussed in Section V.

Even though the phase space factor of Das and Hwa[3] canceled in the particle ratios, the individual single particle distributions of the model

(eq. 4) do agree reasonably well with the data. This comparison is shown in Fig. 6. A summary of our fits to the quark distributions is given in Table II. The quark distributions are plotted in Fig. 7.

IV. PREDICTIONS

With the quark distributions now determined we are now able to predict the final three ratios listed in Table I. We require $\sqrt{s} \gtrsim 10$ GeV where radial scaling has been shown to hold, and we expect these ratios to be accurate at least for $x_R \gtrsim 0.5$.

In Fig. 8 we plot the model predictions for the ratios π^+/K_s^o, π^o/η, and K^+/K_s^o. We note that the π^+/K_s^o ratio rises for increasing x_R. From Table I we see that this ratio is controlled by the $u(x)/d(x)$ ratio at large x_R. Hence the π^+/K_s^o ratio should follow the π^+/π^- ratio. The π^o/η ratio is calculated to be approximately equal to 3. This is expected since $s\bar{s}$ recombination is small relative to $u\bar{u}$ and $d\bar{d}$ recombination. For large $x_R \gtrsim 0.5$ the π^o/η ratio prediction is still approximate since the Das-Hwa model does not allow for π^o-mesons resulting from η decays. Of course for small x_R, we expect the π^o/η ratio to exceed 3 due to the strong contribution of resonance decay to the π^o cross section. The behavior of the K^+/K_s^o ratio is expected to closely follow the behavior of the π^+/π^- ratio since it is again controlled by the $u(x)/d(x)$ ratio.

V. DISCUSSION

A. Momentum Sum Rules

We have found the sea quark x-distributions in the proton by using the quark-antiquark recombination model of Das and Hwa.[3] An interesting result is the large amount of $u-\bar{u}$ and $d-\bar{d}$ sea quarks which we find necessary to fit the data. As we have discussed, this phenomenon is not unexpected. We interpret this enhancement of the sea to imply that there is a significant contribution of the gluons which carry half the proton momentum to the sea quark distributions. This contribution takes place by the gluons converting to $q\bar{q}$ sea pairs and then to mesons. Our analysis leads to the following amounts of momentum carried by the various partons:

$$\int_0^1 xu(x)dx = 0.403,$$

$$\int_0^1 xd(x)dx = 0.257,$$

$$\int_0^1 x\bar{u}(x)dx = \int_0^1 x\bar{d}(x)dx = 0.133,$$

$$\int_0^1 xs(x)dx = \int_0^1 x\bar{s}(x)dx = 0.020,$$

which accounts for 96.6% of the total proton momentum. We regard this nearly total saturation of the proton momentum sum rules as strong support for our intrepretation of the gluons converting to $q-\bar{q}$ pairs thereby giving a large contribution to meson production at low p_T.

B. Low Mass Dileptons

Landshoff and Polkinghorne[13] and Bjorken and Weisberg[14] have suggested that low mass dilepton production should be calculated within the Drell-Yan parton model framework by including the extra wee partons that are produced in hadron collisions. Thus, we believe that the very enhanced sea quark distributions that we find by analyzing hadron fragmentation data should be quite relevant in the production of low mass dileptons.

We have calculated the standard Drell-Yan prediction for μ-pair production at 225 GeV/c using the original Field-Feynman sea distributions[1] and the enhanced sea distributions we have determined. The results are shown in Fig. 9, where we notice that our enchanced sea distributions lead to striking agreement with the data.[15] This suggests that the enhanced quark-antiquark sea, operative in the meson production by quark recombination, also produces a large amount of muon-pairs by quark-antiquark annihilation.

We note that an extrapolation of our enhanced sea calculation to high mass pairs is much larger than the observed μ-pair yield. In fact, the observed yield is predicted quite well by the standard amount of sea quarks. Presumably this means that low mass pairs are produced in the long time interval characteristic of ordinary hadron production, while high mass pairs are produced in a very short time interval. A complete understanding of the transition from the long time scale

process operative in the low mass region to the short time scale process operative in the high mass region would be very interesting, but is unfortunately presently unknown to us.

C. Resonance Contributions

The model of Das and Hwa[3] has made no explicit provision for the effect of resonances on single particle inclusive production. However, the parent-child relationship suppresses resonance decay contributions to inclusive spectra for $x_R \gtrsim 0.5$. Therefore, we believe that our calculations are most relevant in this large x_R kinematic range, as we have emphasized in the analysis.

The effects of resonances are most strongly felt in the low x_R region. For example, if we consider the effect of vector resonances produced with the same cross section as pseudoscalars, then obviously the magnitudes and shapes determined for our sea distributions will change. However, in our analysis we have emphasized as far as possible the data of large x_R in the determination of the sea parameters. For example, the magnitude of the K^+/K^- ratio for $x_R \gtrsim 0.5$ conclusively implies an enhancement of the nonstrange sea, although the exponents n_u and u_d might vary as much as one unit from the favored value 8.

The effects of resonances should contribute most strongly to the π/K ratios at small x_R. We estimate that by including resonance production, we could force $n_s \simeq n_u$ and $s_o/u_o \simeq 0.5$.

VI. SUMMARY

The particle ratios in the model of Das and Hwa[3] provide a sensitive method for determining the quark sea distributions in the proton. This work may obviously be extended to incident pion, kaon, and hyperon beams.[16] We also speculate that quark recombination and the enhanced sea may be important in the understanding of particle production in hadron-nucleus collisions. We find that the effective sea quark distributions relevant to single particle production is enhanced by a factor 10 over the sea determined in lepton experiments. We interpret this enhancement to follow from the significant contribution of the conversion of gluons to quark -antiquark pairs. We find that the data require sea quark distributions, which with the known valence quark distributions, essentially saturate the proton momentum sum rule. We have predicted other particle ratios for $x_R \gtrsim 0.5$. Using the enhanced sea leads to good agreement with low mass muon-pair production in the Drell-Yan model.

In conclusion, we note that hadron production in the fragmentation region is a very useful probe of the quark structure of colliding hadrons. Therefore, more detailed and sophisticated investigations along these lines are likely to be especially fruitful and rewarding.[16]

ACKNOWLEDGMENTS

We wish to thank many of our colleagues at Fermilab; most especially H. Miettinen, for many very helpful and interesting discussions. We are also aware of other works by J. Ranft[17] and T. DeGrand and H. Miettinen[18] which complement the present work.

REFERENCES

[1] R. D. Field and R. P. Feynman, Phys. Rev. D15, 2590 (1977).

[2] W. Ochs, Nucl. Phys. B118, 397 (1977).

[3] K. P. Das and Rudolph Hwa, Phys. Letters 68B, 459 (1977).

[4] J. R. Johnson et al. submitted to Phys. Rev. D. These data have been averaged over p_T ($0.25 \leq p_T \leq 1.5$ GeV/c) since no systematic p_T dependence over this range is observed.

[5] Many authors have considered the quark-antiquark recombination mechanism. Prior to the papers by Ochs (Ref. 2) and Das and Hwa (Ref. 3) we note the works of V. V. Anisovich and V. M. Shekhter Nucl. Phys. B55, 455 (1973) and J. D. Bjorken and G. Farrar, Phys. Rev. D9, 1449 (1974).

[6] This point has been emphasized to us by H. Miettinen (private communication).

[7] P. Cappiluppi et al., Nucl. Phys. B79, 189 (1974). Only data at $p_T \leq 0.5$ GeV/c have been used.

[8] M. G. Albrow et al., Nucl. Phys. B56, 333 (1973) and Nucl. Phys. B73, 40 (1974). Only data for $p_T \leq 0.5$ GeV/c have been used.

[9] F. E. Taylor et al., Phys. Rev. D14, 1217 (1976).

[10] D. W. Duke, Phys. Rev. D11, 43 (1975).

[11] J. C. Sens (private communication).

[12] D. Antreasyan et al., Phys. Rev. Lett. 38, 112 (1977) and 38, 115 (1977).

[13] P. V. Landshoff and J. C. Polkinghorne, Nucl. Phys. B33, 221 (1971).

[14] J. D. Bjorken and H. Weisberg. Phys. Rev. D13, 1405 (1976).

[15] K. J. Anderson et al., (submitted to XVIII Conference in High Energy Physics, Tbilisi, USSR, (1976); J. G. Branson et al., Phys. Rev. Lett. 38, 1334 (1977).

[16] Work in progress. (T. DeGrand, D. Duke, T. Inami, H. Miettinen, J. Ranft, H. Thacker).

[17] J. Ranft, SLAC Report (to be published).

[18] T. A. DeGrand and H. I. Miettinen, SLAC Report (to be published).

TABLE CAPTIONS

Table I. The formulae for various particle ratios are listed from the model of Das and Hwa (Ref. 3). The functions $F_q(x)$ are the probabilities for finding a quark q with a momentum fraction x of the proton. For example $F_u(x) = xu_v(x) + xu_{sea}(x)$, where $xu_v(x)$ is the valence sea distribution determined by Field and Feynman (Ref. 1) and $xu_{sea}(x)$ is the sea distribution determined by this analysis.

Table II. The results of our fits to the sea distributions are given. $xu_v(x)$ is the valence distribution from Field and Feynman (Ref. 1) etc. We see that the x dependence of the strange sea is less steep than the x dependence of the non-strange sea.

Table I.

$$\frac{\pi^+}{\pi^-}(x) = \frac{\alpha_{\pi^+}\beta_{\pi^+} \int_0^x F_u(x_1)\, F_{\bar{d}}(x-x_1)\, dx_1}{\alpha_{\pi^-}\beta_{\pi^-} \int_0^x F_d(x_1)\, F_{\bar{u}}(x-x_1)\, dx_1}$$

$$\frac{K^+}{K^-}(x) = \frac{\alpha_{K^+}\beta_{K^+} \int_0^x F_u(x_1)\, F_{\bar{s}}(x-x_1)\, dx_1}{\alpha_{K^-}\beta_{K^-} \int_0^x F_s(x_1)\, F_{\bar{u}}(x-x_1)\, dx_1}$$

$$\frac{\pi^-}{K^-}(x) = \frac{\alpha_{\pi^-}\beta_{\pi^-} \int_0^x F_d(x_1)\, F_{\bar{u}}(x-x_1)\, dx_1}{\alpha_{K^-}\beta_{K^-} \int_0^x F_s(x_1)\, F_{\bar{u}}(x-x_1)\, dx_1}$$

$$\frac{\pi^+}{K^+}(x) = \frac{\alpha_{\pi^+}\beta_{\pi^+} \int_0^x F_u(x_1)\, F_{\bar{d}}(x-x_1)\, dx_1}{\alpha_{K^+}\beta_{K^+} \int_0^x F_u(x_1)\, F_{\bar{s}}(x-x_1)\, dx_1}$$

$$\frac{\pi^+}{K_s^o}(x) = \frac{\alpha_{\pi^+}\beta_{\pi^+} \int_0^x F_u(x_1)\, F_{\bar{d}}(x-x_1)\, dx_1}{\alpha_{K_s}\beta_{K_s} \int_0^x \frac{1}{2}\left(F_d(x_1)\, F_{\bar{s}}(x-x_1) + F_s(x_1)\, F_{\bar{d}}(x-x_1)\right) dx_1}$$

$$\frac{\pi^o}{\eta}(x) = \frac{\alpha_{\pi^o}\beta_{\pi^o} \int_0^x \frac{1}{2}\left(F_u(x_1)\, F_{\bar{u}}(x-x_1) + F_d(x_1)\, F_{\bar{d}}(x-x_1)\right) dx_1}{\alpha_\eta\beta_\eta \int_0^x \frac{1}{6}\left(F_u(x_1)\, F_{\bar{u}}(x-x_1) + F_d(x_1)\, F_{\bar{d}}(x-x_1) + 4\, F_s(x_1)\, F_{\bar{s}}(x-x_1)\right) dx_1}$$

$$\frac{K^+}{K_s^o}(x) = \frac{\alpha_{K^+}\beta_{K^+} \int_0^x F_u(x_1)\, F_{\bar{s}}(x-x_1)\, dx_1}{\alpha_{K_s}\beta_{K_s} \int_0^x \frac{1}{2}\left(F_d(x_1)\, F_{\bar{s}}(x-x_1) + F_s(x_1)\, F_{\bar{d}}(x-x_1)\right) dx_1}$$

Table II.

$$xu(x) = xu_V(x) + x\bar{u}(x)$$

$$xd(x) = xd_V(x) + x\bar{d}(x)$$

$$x\bar{u}(x) = x\bar{d}(x) = 1.2\ (1 - x)^8$$

$$xs(x) = x\bar{s}(x) = 0.135(1 - x)^{5.75}$$

FIGURE CAPTIONS

Fig. 1: a) The production of a π^+ meson by a quark fragmentation mechanism is shown. It is important to note that the x values of the pion ($x_\pi = x_1 - x_2$) is less than that of the fragmenting u quark. Hence this process is suppressed at large x_π.

b) Shown is the quark-antiquark recombination mechanism for π^+ production. We see that the x_π value ($x_\pi = x_1 + x_2$) is larger than either x values of the quark or antiquark. Hence this process can produce mesons at large x with a higher probability than the quark fragmentation process.

c) π^+ production via gluon fragmentation is shown. As in the case of quark fragmentation, the pion x value is less than the x value of the fragmenting gluon.

d) The long time scale ΔT operative in meson production in the fragmentation region versus the short time scale Δt of deep inelastic lepton scattering is illustrated. This long time allows a significant fraction of the gluons to convert to

quark-antiquark pairs and hence to contribute to meson production.

Fig. 2: The π^+/π^- ratio is plotted versus x_R for Fermilab data (Ref. 4) and ISR data (Ref. 7 and 8). Several choices of the sea exponents n_u, n_d are shown for $u_o = d_o$.

Fig. 3: The K^+/K^- ratio is shown versus x_R. The line through the data represents our fit obtained by setting $u_o = d_o = 1.2$ and $n_s = 5.75$.

Fig. 4: The π^-/K^- ratio is plotted versus x_R. The line through the data is our fit obtained by setting $s_o = 0.135$ having fixed $u_o = d_o = 1.2$, $n_u = n_d = 8.0$ and $n_s = 5.75$.

Fig. 5: The π^+/K^+ ratio versus x_R is shown. Although this ratio is determined by the previous 3 ratios, it is interesting to observe the decrease of this ratio for increasing x_R. This is due to our choice of setting $n_s < n_u = n_d$.

Fig. 6: The invariant cross sections for fixed $p_T = 0.25\,\mathrm{GeV/c}$ from Ref. 4 are shown. The lines through the data are the calculated x_R dependencies of the model of Das and Hwa. Resonable agreement with the data is obtained.

Fig. 7: The determined quark distributions are plotted versus x. For example, xu(x) is the sum of the valence sea distribution $xu_v(x)$ taken from Field and Feynman (Ref. 1) and the sea distribution $x\bar{u}(x)$ we have determined. The enhancement of the sea $x\bar{u}(x) = x\bar{d}(x)$ is clearly shown.

Fig. 8: The predicted particle ratios are shown versus x_R. (We have plotted these ratios for the entire x_R range but emphasize that we expect these predictions to hold for $x_R \gtrsim 0.5$.)

Fig. 9: The cross section for $\mu^+\mu^-$ pairs versus the mass $M_{\mu\mu}$ is shown for the data of Ref. 15. Our calculation of the Drell-Yan cross section with our enhanced sea is shown as the solid line. The dotted line is the Drell-Yan cross section for the Field and Feynman (Ref. 1) sea distributions. Both calculations use the measured A dependence.

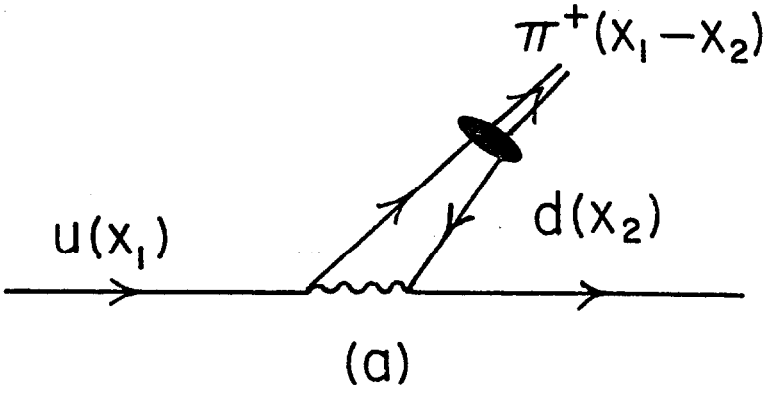

(a)

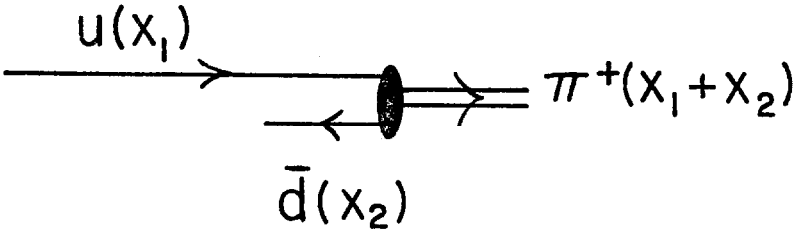

(b)

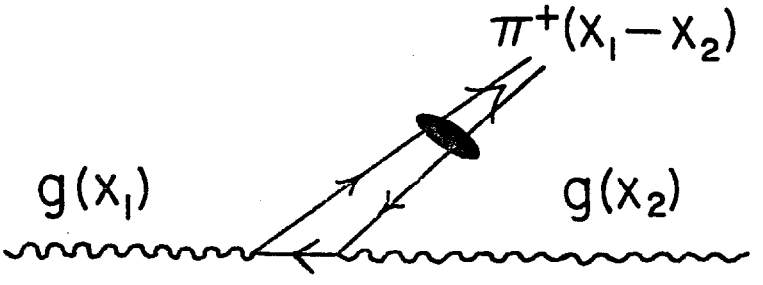

(c)

Fig. 1a,b,c

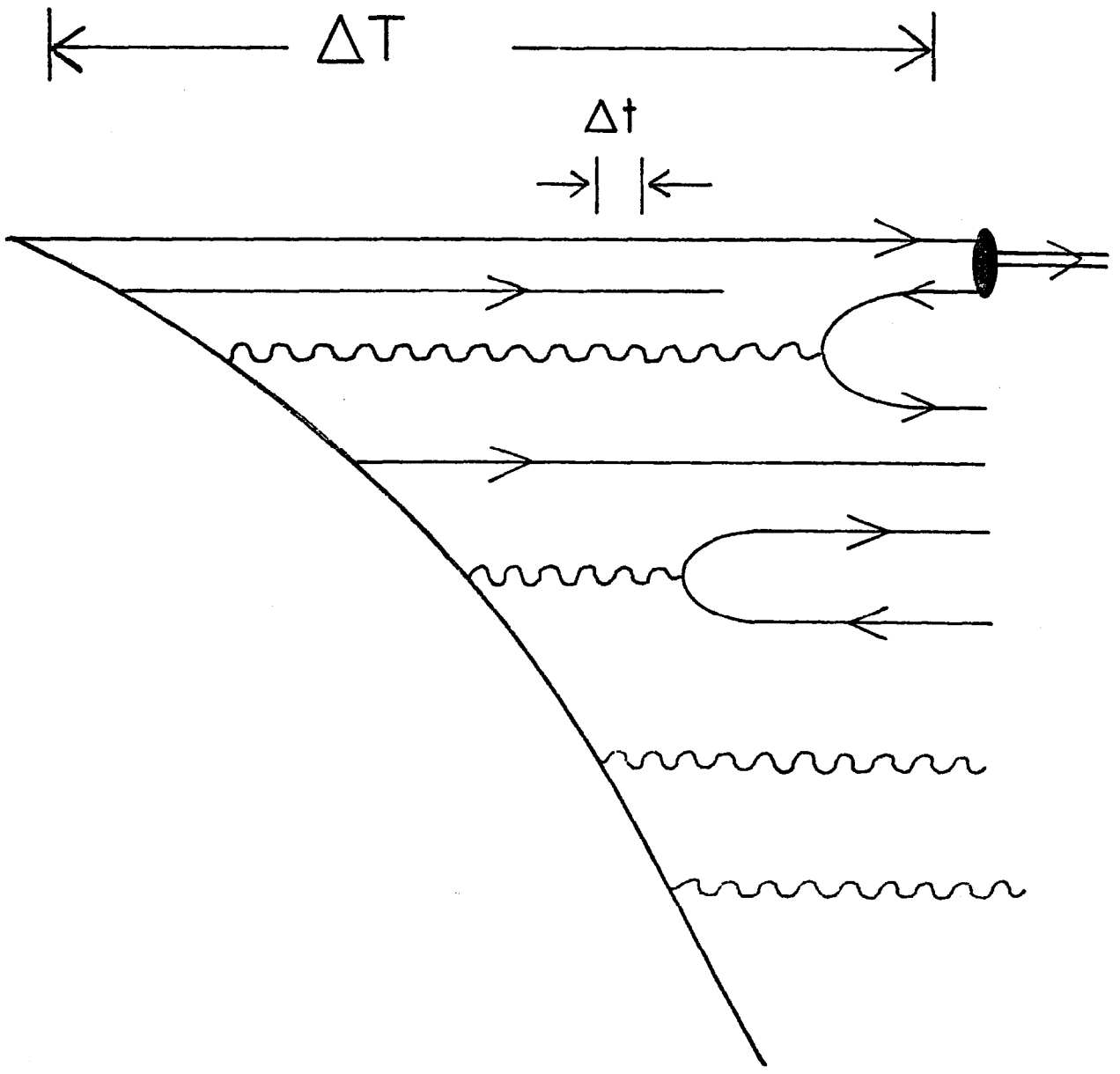

(d)

Fig. 1d

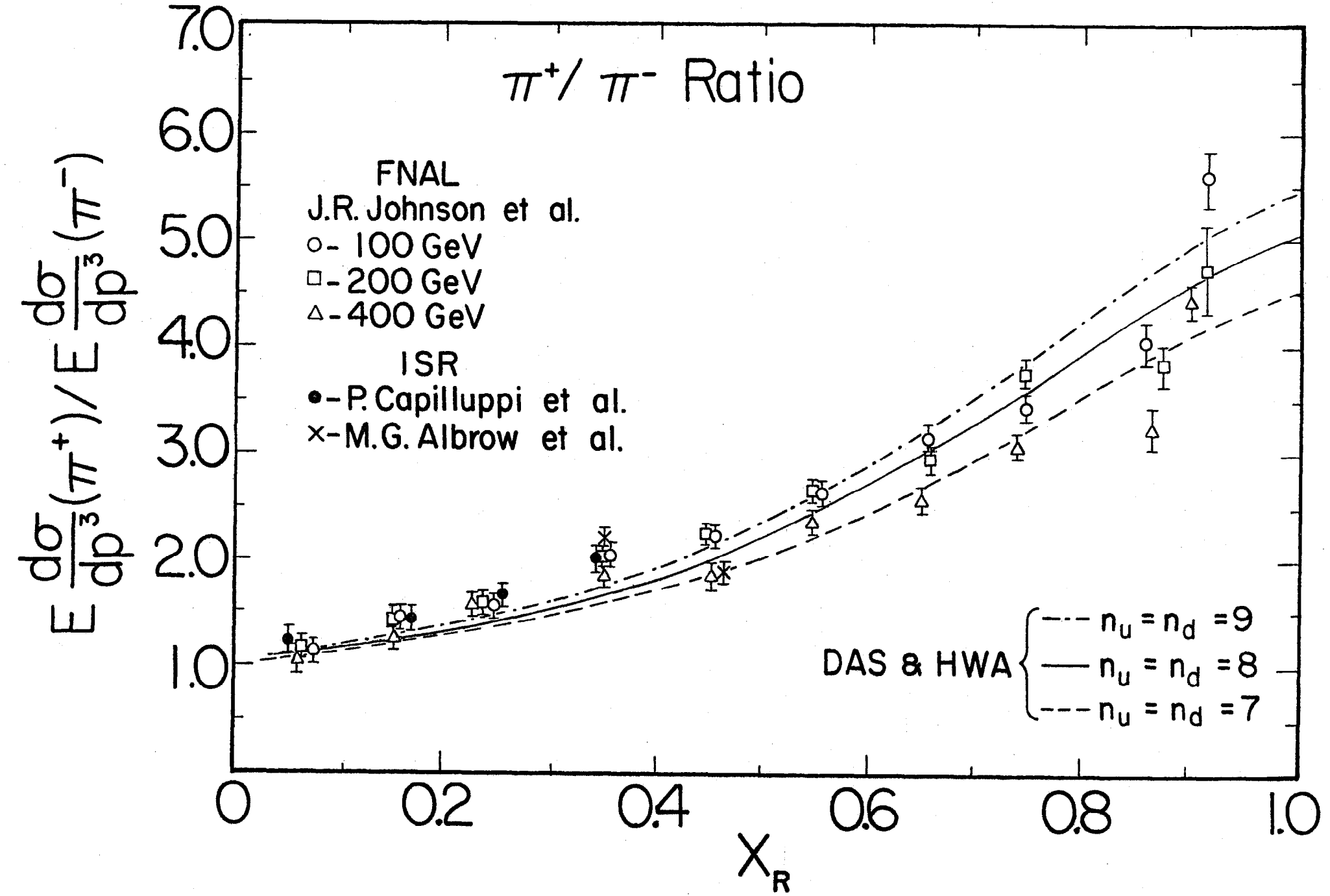
π^+/π^- Ratio
FNAL
J.R. Johnson et al.
○- 100 GeV
□- 200 GeV
△- 400 GeV
ISR
●- P. Capilluppi et al.
×- M.G. Albrow et al.
DAS & HWA
$n_u = n_d = 9$
$n_u = n_d = 8$
$n_u = n_d = 7$
$E\frac{d\sigma}{dp^3}(\pi^+)/E\frac{d\sigma}{dp^3}(\pi^-)$
X_R
7.0
6.0
5.0
4.0
3.0
2.0
1.0
0
0.2
0.4
0.6
0.8
1.0

Fig. 2

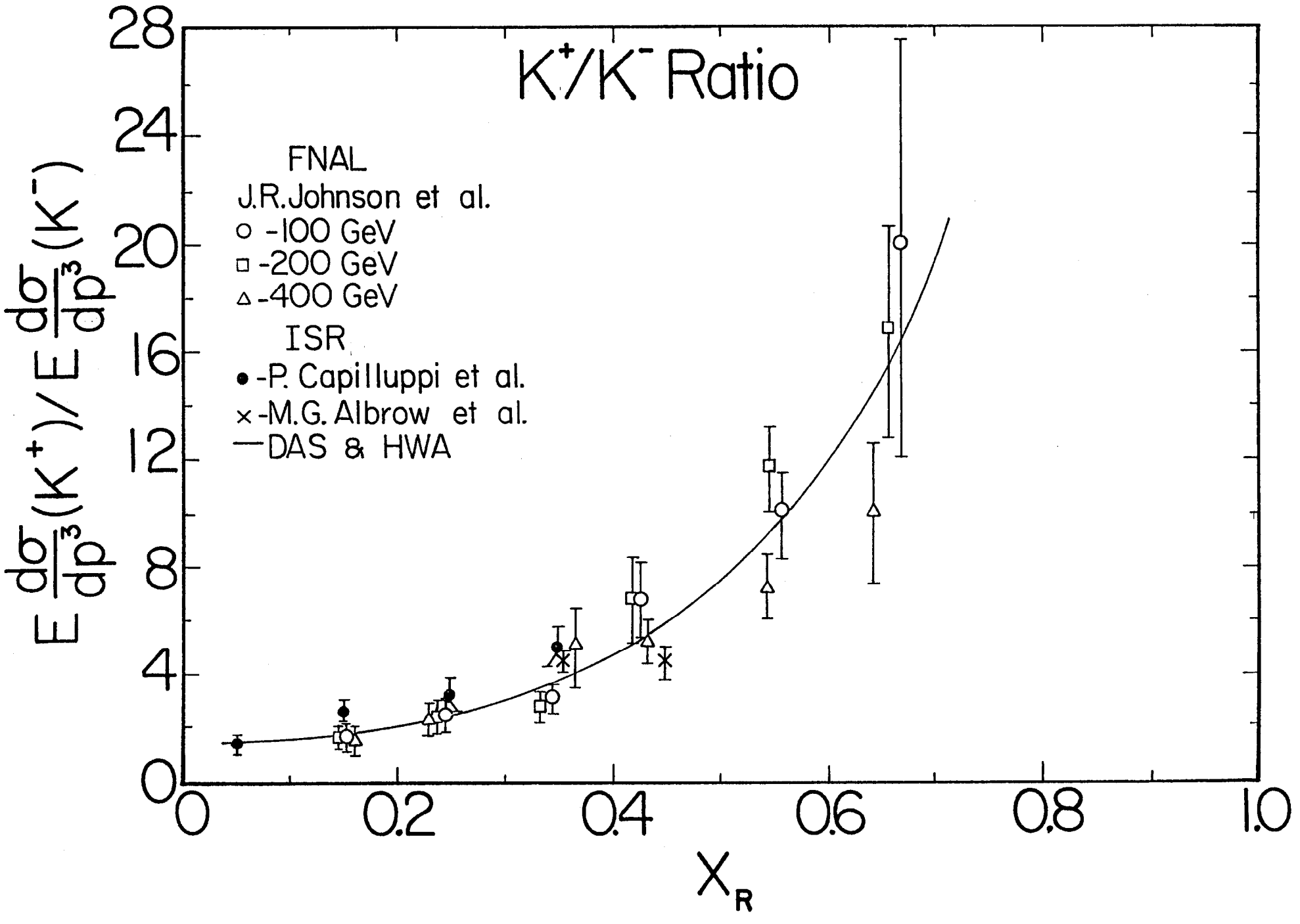
K+/K- Ratio
FNAL
J.R.Johnson et al.
○ -100 GeV
□ -200 GeV
△ -400 GeV
ISR
● -P. Capiluppi et al.
× -M.G. Albrow et al.
— DAS & HWA
E dσ/dp³ (K+)/ E dσ/dp³ (K-)
0
4
8
12
16
20
24
28
0
0.2
0.4
0.6
0.8
1.0
XR

Fig. 3

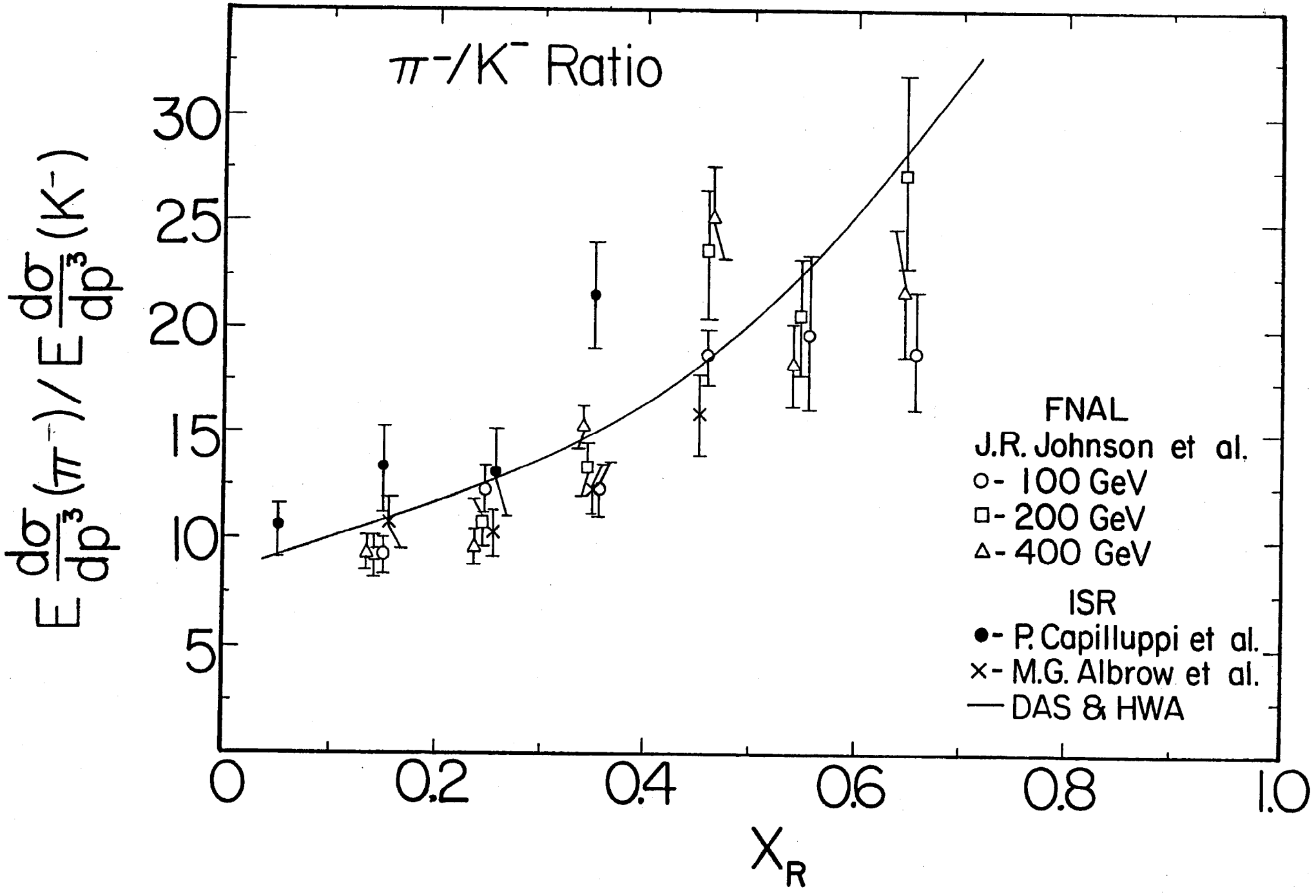
π⁻/K⁻ Ratio
$E\frac{d\sigma}{dp^3}(\pi^-)/E\frac{d\sigma}{dp^3}(K^-)$
30
25
20
15
10
5
0
0.2
0.4
0.6
0.8
1.0
X_R
FNAL
J.R. Johnson et al.
○- 100 GeV
□- 200 GeV
△- 400 GeV
ISR
●- P. Capilluppi et al.
×- M.G. Albrow et al.
— DAS & HWA

Fig. 4

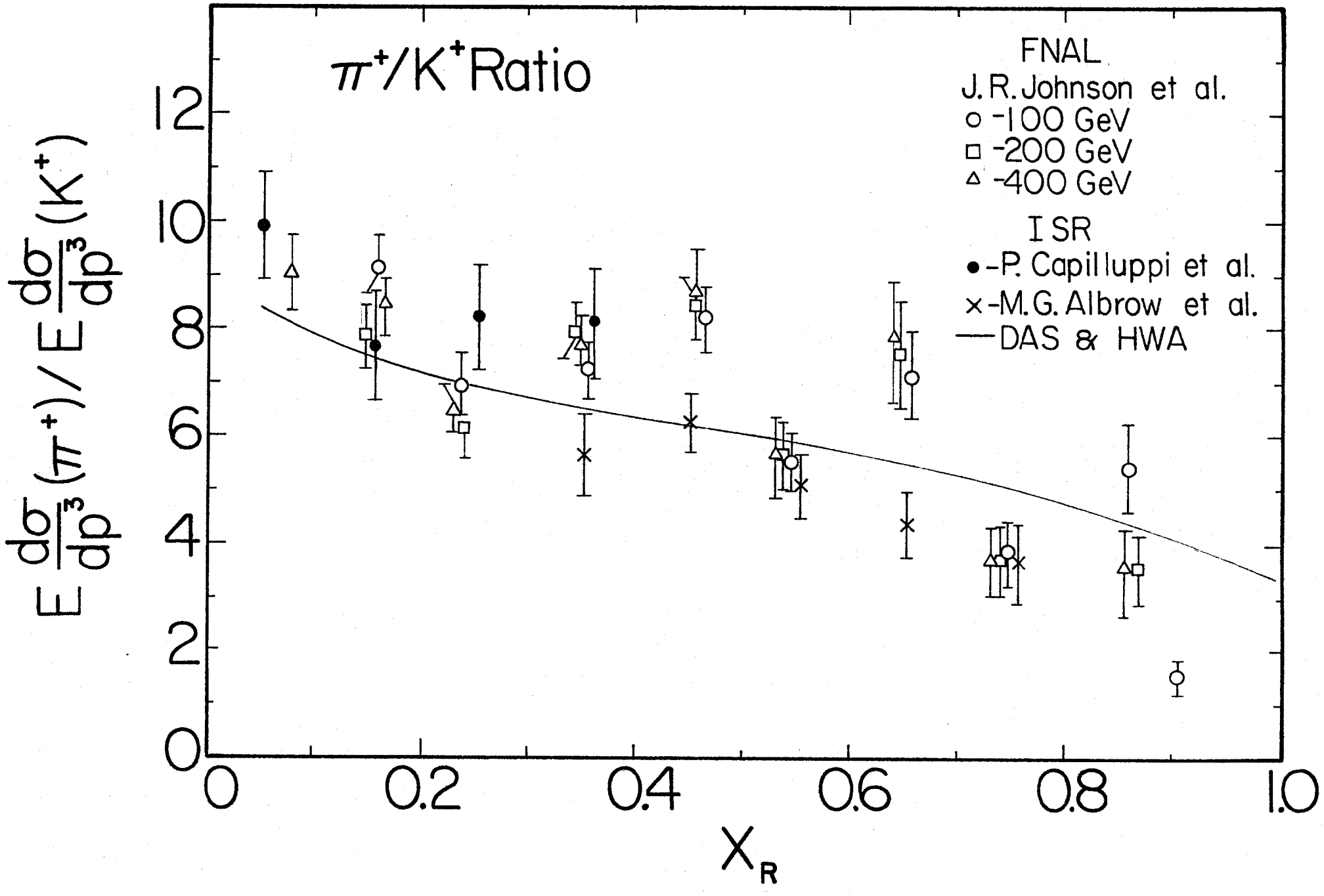
π^+/K^+ Ratio
FNAL
J.R. Johnson et al.
○ -100 GeV
□ -200 GeV
△ -400 GeV
ISR
● -P. Capilluppi et al.
× -M.G. Albrow et al.
— DAS & HWA
$E\frac{d\sigma}{dp^3}(\pi^+) / E\frac{d\sigma}{dp^3}(K^+)$
X_R
0
2
4
6
8
10
12
0
0.2
0.4
0.6
0.8
1.0

Fig. 5

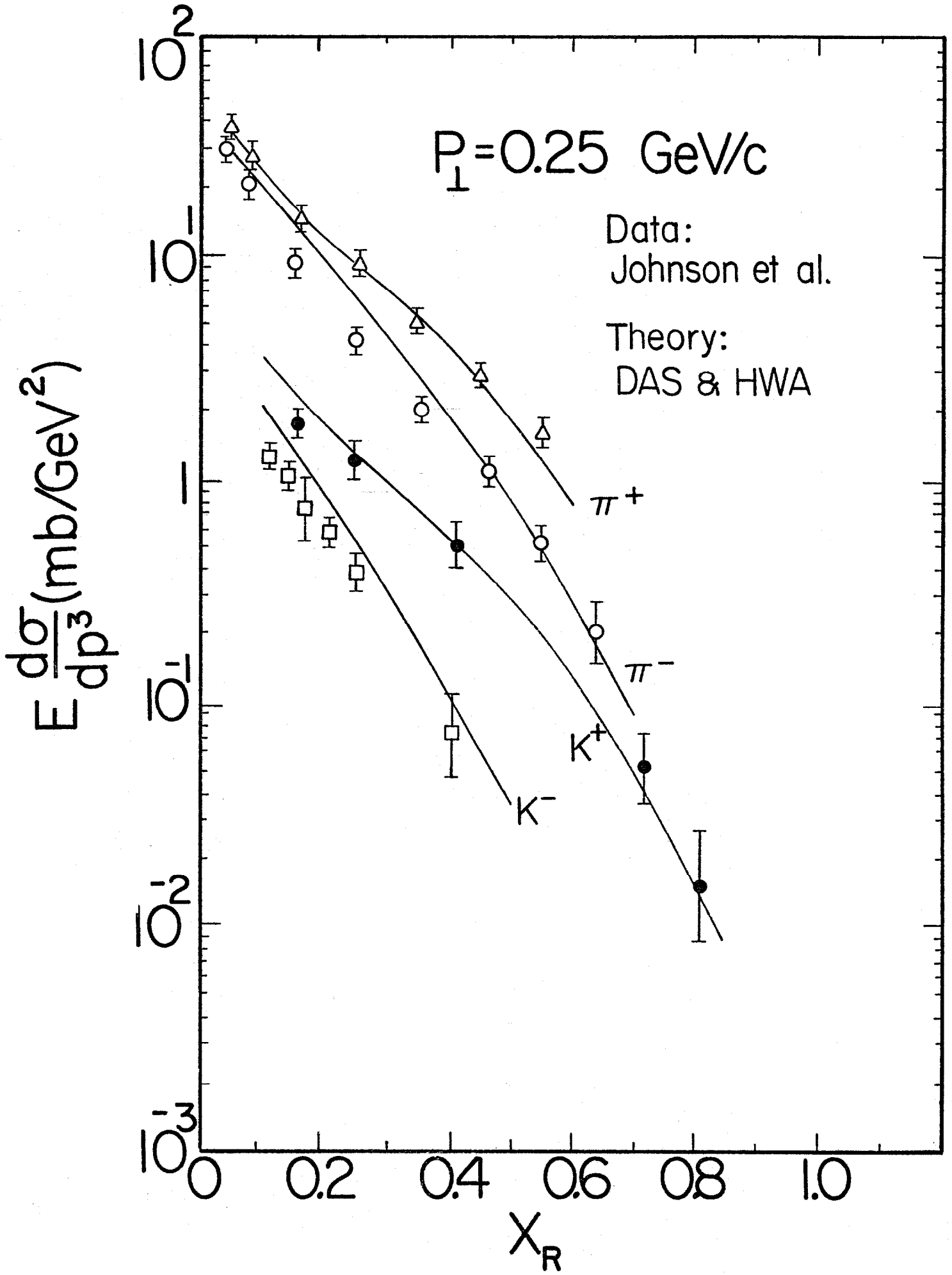
$P_\perp$=0.25 GeV/c
Data:
Johnson et al.
Theory:
DAS & HWA
π^+
π^-
K^+
K^-
$E\frac{d\sigma}{dp^3}$(mb/GeV^2)
10^2
10^1
1
10^{-1}
10^{-2}
10^{-3}
0
0.2
0.4
0.6
0.8
1.0
X_R

Fig. 6

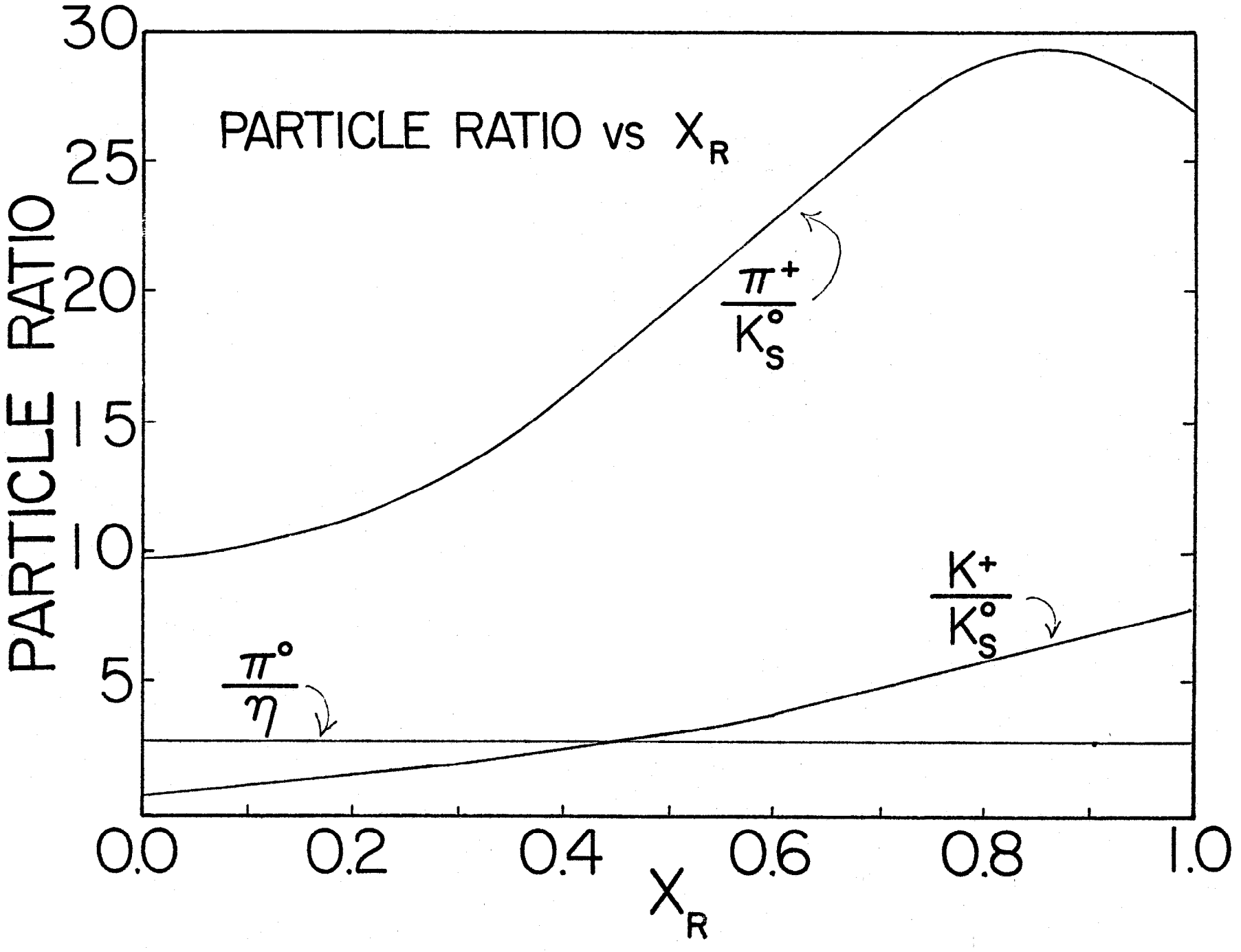
PARTICLE RATIO vs X_R
PARTICLE RATIO
30
25
20
15
10
5
0.0
0.2
0.4
0.6
0.8
1.0
X_R
$\frac{\pi^+}{K_S^\circ}$
$\frac{K^+}{K_S^\circ}$
$\frac{\pi^\circ}{\eta}$

Fig. 7

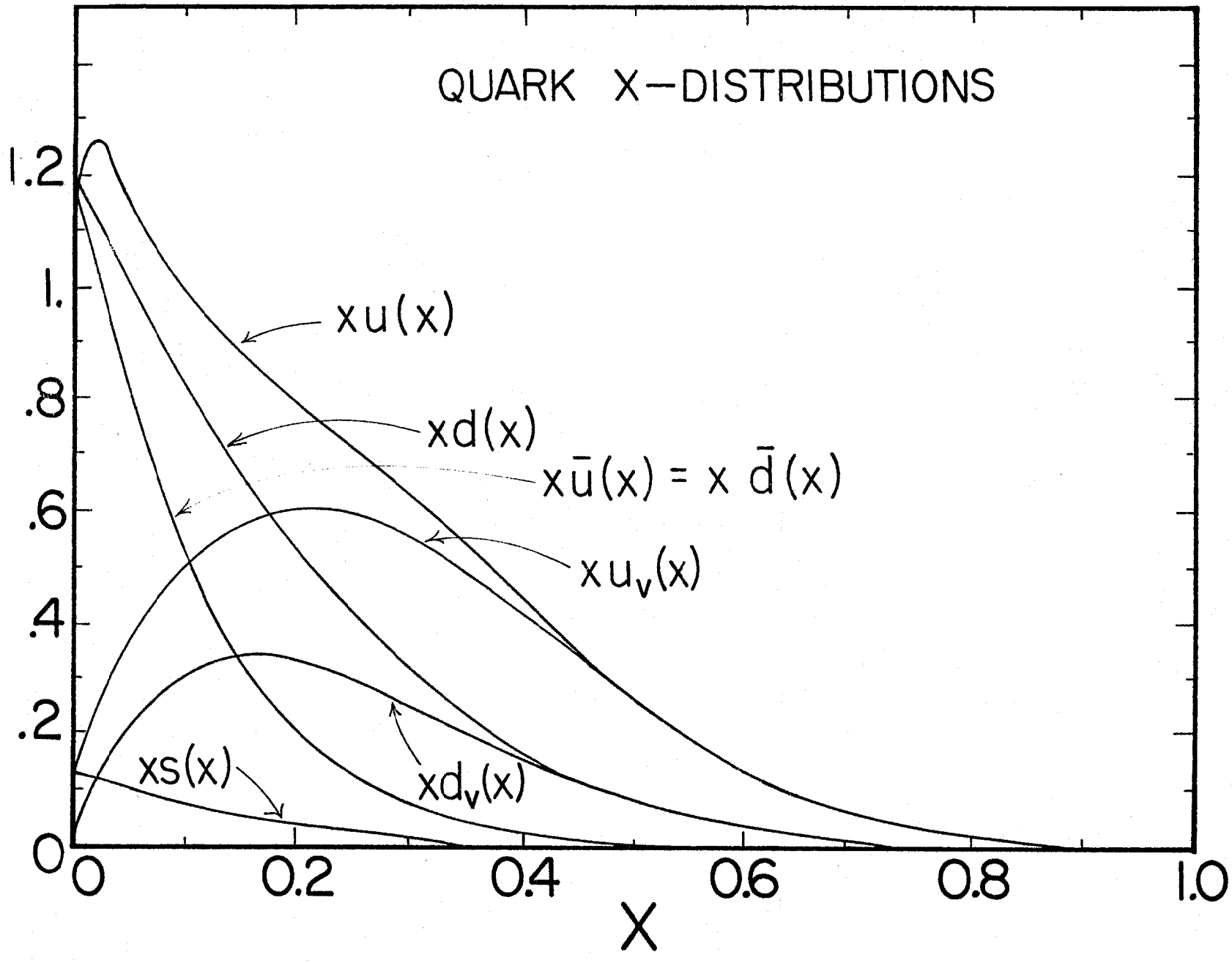
QUARK X-DISTRIBUTIONS
1.2
1.
.8
.6
.4
.2
0
0
0.2
0.4
0.6
0.8
1.0
X
xu(x)
xd(x)
xū(x) = x d̄(x)
xu_v(x)
xs(x)
xd_v(x)

Fig. 8

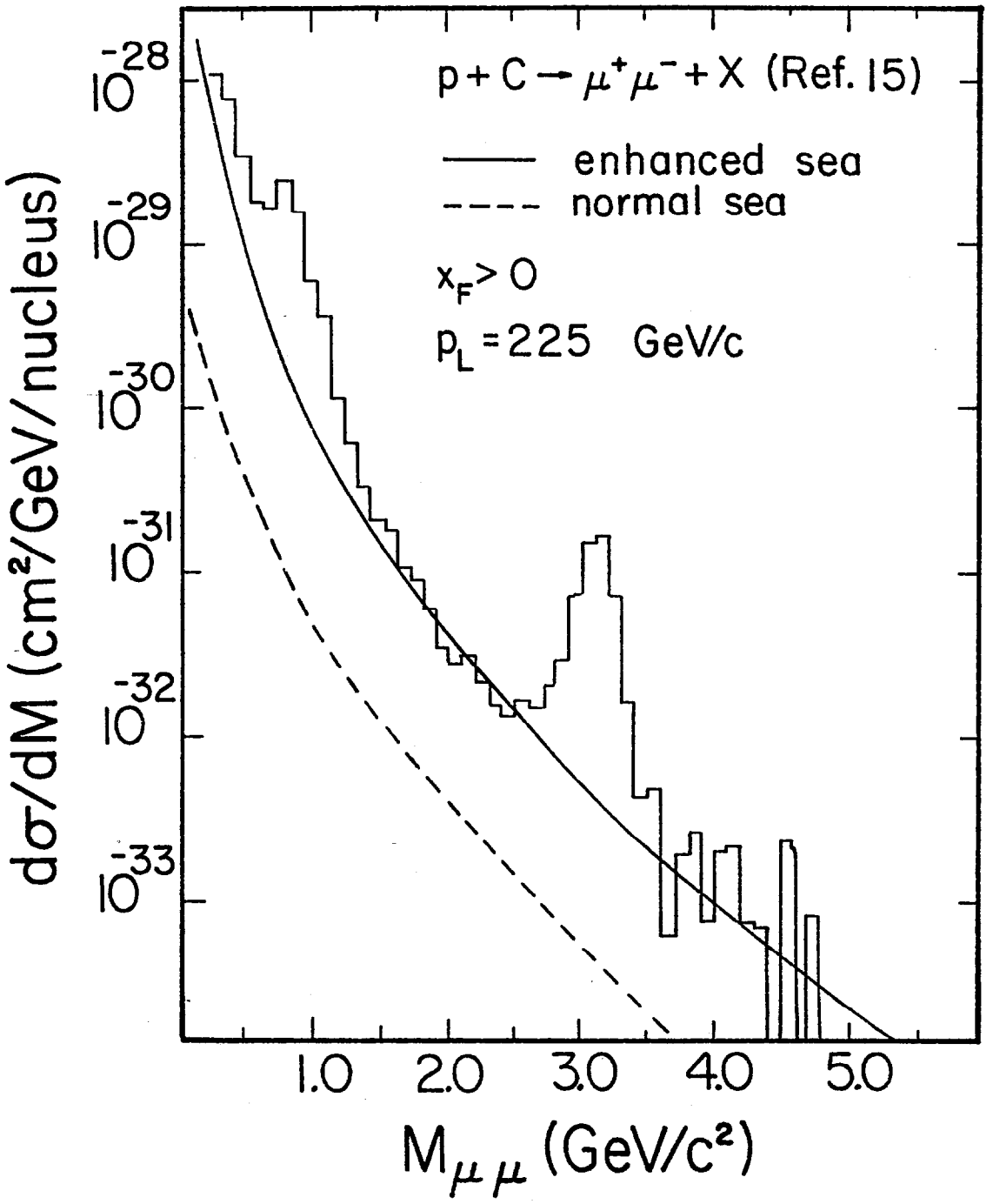
p + C → μ⁺μ⁻ + X (Ref. 15)
enhanced sea
normal sea
$x_F > 0$
$p_L = 225$ GeV/c
$d\sigma/dM$ (cm²/GeV/nucleus)
10^{-28}
10^{-29}
10^{-30}
10^{-31}
10^{-32}
10^{-33}
1.0
2.0
3.0
4.0
5.0
$M_{\mu\mu}$ (GeV/c²)

Fig. 9